# The Active Form of the *Saccharomyces cerevisiae* Ribonucleotide Reductase Small Subunit Is a Heterodimer *in Vitro* and *in Vivo*†

Deborah L. Perlstein,‡,§ Jie Ge,||,§ Allison D. Ortigosa,§ John H. Robblee,§ Zhen Zhang,⊥ Mingxia Huang,⊥ and JoAnne Stubbe*,§

*Departments of Chemistry and Biology, Massachusetts Institute of Technology, Cambridge, Massachusetts 02139, and Department of Biochemistry and Molecular Genetics, University of Colorado Health Sciences Center, Aurora, Colorado 80045*

*Received August 13, 2005; Revised Manuscript Received September 15, 2005*

ABSTRACT: The class I ribonucleotide reductases (RNRs) are composed of two homodimeric subunits: R1 and R2. R2 houses a diferric-tyrosyl radical (Y•) cofactor. *Saccharomyces cerevisiae* has two R2s: Y2 ($\beta_2$) and Y4 ($\beta'_2$). Y4 is an unusual R2 because three residues required for iron binding have been mutated. While the heterodimer ($\beta\beta'$) is thought to be the active form, several *rnr4*Δ strains are viable. To resolve this paradox, N-terminally epitope-tagged $\beta$ and $\beta'$ were expressed in *E. coli* or integrated into the yeast genome. *In vitro* exchange studies reveal that when apo-($His_6$)-$\beta_2$ ($^{His}\beta_2$) is mixed with $\beta'_2$, apo-$^{His}\beta\beta'$ forms quantitatively within 2 min. In contrast, holo-$\beta\beta'$ fails to exchange with apo-$^{His}\beta_2$ to form holo-$^{His}\beta\beta$ and $\beta'_2$. Isolation of genomically encoded tagged $\beta$ or $\beta'$ from yeast extracts gave a 1:1 complex of $\beta$ and $\beta'$, suggesting that $\beta\beta'$ is the active form. The catalytic activity, protein concentrations, and Y• content of the *rnr4*Δ and wild type (wt) strains were compared to clarify the role of $\beta'$ *in vivo*. The Y• content of *rnr4*Δ is 15-fold less than that of wt, consistent with the observed low activity of *rnr4*Δ extracts (<0.01 nmol $min^{-1}$ $mg^{-1}$) versus wt (0.06 ± 0.01 nmol $min^{-1}$ $mg^{-1}$). $^{FLAG}\beta_2$ isolated from the *rnr4*Δ strain has a specific activity of 2 nmol $min^{-1}$ $mg^{-1}$, similar to that of reconstituted apo-$^{His}\beta_2$ (10 nmol $min^{-1}$ $mg^{-1}$), but significantly less than holo-$^{His}\beta\beta'$ (∼2000 nmol $min^{-1}$ $mg^{-1}$). These studies together demonstrate that $\beta'$ plays a crucial role in cluster assembly *in vitro* and *in vivo* and that the active form of the yeast R2 is $\beta\beta'$.

Ribonucleotide reductases (RNRs)[1] catalyze the conversion of ribonucleotides to deoxyribonucleotides, providing the monomeric precursors for DNA replication and repair (*1*). The class I RNRs are composed of a large subunit, R1, and a small subunit, R2. R1 contains the site of nucleotide reduction and the allosteric effector binding sites that control the rate and the specificity of nucleotide reduction. R2 houses the diferric-tyrosyl radical (Y•) cofactor required for RNR activity. The budding yeast *Saccharomyces cerevisiae* has two R2 genes: *RNR2* and *RNR4*. *RNR2* is essential and the corresponding protein, designated Y2 or $\beta_2$,[2] is a homodimer containing the essential residues conserved in all R2s that are required to form the cofactor (*2*, *3*). *RNR4*, however, is essential for viability only in some genetic backgrounds (*4*−*6*). The protein, designated Y4 or $\beta'_2$, is a homodimer and has substitutions in three of the six conserved amino acids required for iron binding (*5*, *6*).

Recent studies from several labs have suggested that the active form of R2 in *S. cerevisiae* is a heterodimer ($\beta\beta'$) composed of one protomer of Y2 and one of Y4 (*7*−*9*). Only $\beta$ can form the essential diferric-Y• cofactor, and thus, there is a maximum of 1 Y•/$\beta\beta'$ (*2*, *3*). Previously, our laboratory has demonstrated that $\beta'$ is required to generate the diferric-Y• cofactor of $\beta$ *in vitro*, and Thelander and co-workers have proposed, on the basis of their inability to isolate active R2 unless *RNR2* and *RNR4* were coexpressed in *Escherichia coli*, that $\beta\beta'$ is the active form of yeast R2 (*7*−*9*). However, the paradox of the viability of several *rnr4*Δ strains remains and has led us to further investigate the role of $\beta'$ and the active form of yeast R2 *in vitro* and *in vivo*.

Two proposals for the role of $\beta'$ *in vivo* have been put forth: that of an iron chaperone for $\beta$ and that of a stoichiometric folding chaperone for $\beta$ (*8*, *9*). The proposal

† D.L.P. and A.D.O. were supported in part by the NIH training grant 5T32 CA 09112-28. J.S. acknowledges support of the NIH (GM29595). M.H. acknowledges support of the NIH (CA095207) and the ACS (0305001GMC).

* To whom correspondence should be addressed. Telephone: (617) 253-1814. Fax: (617) 258-7247. E-mail: stubbe@mit.edu.

‡ Present address: Department of Microbiology and Molecular Genetics, Harvard Medical School, Boston, MA 02115.

§ Massachusetts Institute of Technology.

|| Present address: Infinity Pharmaceuticals, Cambridge, MA 02139.

⊥ University of Colorado Health Sciences Center.

[1] Abbreviations: Abs, antibodies; AEBSF, 4-(2-aminoethyl)benzenesulphonyl fluoride; α, polypeptide encoded by *RNR1*; α′, polypeptide encoded by *RNR3*; $\beta$, polypeptide encoded by *RNR2*; $\beta'$, polypeptide encoded by *RNR4*; CD, circular dichroism; DSC, differential scanning calorimetry; E-64, (2*S*,3*S*)-3-(*N*-{(*S*)-1-[*N*-(4-guanidinobutyl)carbamoyl]3-methylbutyl}carbamoyl)oxirane-2-carboxylic acid; FT, flow through; PBS, phosphate-buffered saline; R1, ribonucleotide reductase large subunit; R2, ribonucleotide reductase small subunit; *RNR1* and *RNR3*, yeast RNR large subunit genes; *RNR2* and *RNR4*, yeast RNR small subunit genes; RNR, ribonucleotide reductase; SC-Ura, synthetic complete media without uracil; wt, wild type; Y•, tyrosyl radical; Y1, α; Y2, $\beta_2$; Y3, α′; Y4, $\beta'_2$.

[2] The nomenclature for naming the yeast RNR proteins differs from that in our previous publications in an effort to clarify the quaternary structures of these subunits.

10.1021/bi051616+ CCC: $30.25 
Published on Web 10/21/2005

that $\beta'$ is an iron chaperone was inspired by the discovery of a copper chaperone protein required for copper delivery to the copper−zinc superoxide dismutase (*10*−*12*). The observation that the diferric-Y· cofactor of $\beta$ could not be reconstituted *in vitro* unless $\beta'$ was also present supported this hypothesis (*9*). However, a 1:1 ratio of $\beta_2/\beta'_2$ is required to obtain protein with maximal activity for nucleotide reduction, and the $\beta\beta'$ is stable, indicating that $\beta'_2$ is not acting catalytically in the activation of $\beta_2$ *in vitro* (*7*). Additionally, experiments to demonstrate $Fe^{2+}$ or $Fe^{3+}$ binding to $\beta'_2$ have not been successful (*7*).

The proposal that $\beta'$ is a stoichiometric folding chaperone (*8*) is not consistent with our successful expression and isolation of a hexa-histidine-tagged version of $\beta_2$ ($^{His}\beta_2$) in the absence of $\beta'_2$ (*7*). Furthermore, a crystal structure of the apo-$^{His}\beta_2$ has been solved, revealing that it is folded and structurally homologous to other R2s (*13*). These results argue against the folding chaperone hypothesis. Thus, the biochemical evidence is inconsistent with both proposed roles for $\beta'_2$, and neither proposal explains the viability of the *rnr4*Δ strains.

Recently, a new model for the role of $\beta'_2$ was proposed on the basis of the crystal structures of the apo-$^{His}\beta_2$ and $\beta'_2$ in comparison with the structure of the partially Zn-loaded $^{His}\beta\beta'$ (*13*, *14*). This comparison reveals that helix αB of $\beta$, which houses Asp145 that binds to Fe1, converts from a disordered state in $\beta_2$ to an ordered state in $\beta\beta'$. These observations suggested that $\beta'$ stabilizes a local conformation of $\beta$ to facilitate cofactor assembly. The caveat with this model, however, is that $\beta\beta'$ was crystallized at pH 4.9 and does not have an assembled cofactor.

Structural and biochemical experiments have established that the $\beta\beta'$ is an active R2 *in vitro*. Two observations made soon after the discovery of *RNR4*, however, seemed to contradict the hypothesis that $\beta\beta'$ is the active yeast R2 *in vivo*. The first was that immunolocalization studies using overexpressed N-terminally epitope-tagged RNR proteins revealed that $\beta$ was localized predominantly to the cytoplasm, while $\beta'$ was localized predominantly to the nucleus (*6*). Recently, however, the subcellular localization of $\beta$ and $\beta'$ was reinvestigated using polyclonal antibodies (Abs) to $\beta$ and $\beta'$ (*15*). These new experiments established that $\beta$ and $\beta'$ are co-localized to the nucleus and undergo a nucleus to cytoplasm redistribution in response to a need for biosynthesis of deoxynucleotides during DNA replication or repair. Thus, the subcellular localization patterns of $\beta$ and $\beta'$ no longer contradict the hypothesis that $\beta\beta'$ is the active form of the yeast R2.

The second observation that contradicts the essential role of $\beta\beta'$ was the fact that deletion of *RNR4* is not lethal in some strain backgrounds (*4*, *5*). While these strains grow slowly, they must still be capable of making deoxynucleotides to support cell division; thus, $\beta_2$ must be an active form of yeast R2 in these strains.

Here, we present experiments that provide further support for the hypothesis that the $\beta\beta'$ is the active form of yeast R2 *in vitro* and to further examine the active form of R2 *in vivo*. Several experiments utilizing $^{His}\beta_2$, $^{His}\beta\beta'$, $^{HA}\beta'_2$, and $\beta\beta'$ have allowed us to demonstrate that, while the apo forms of these R2s are capable of exchanging their protomers, assembly of the diferric-Y· cofactor prevents exchange. Re-examination of cofactor assembly with $^{His}\beta_2$, with a focus on the lower limit of detection for Y· and nucleotide reductase activity, revealed that an active homodimer of $^{His}\beta_2$ can form with a specific activity 200-fold lower than that of $^{His}\beta\beta'$. A comparison of *S. cerevisiae* wt and *rnr4*Δ strains for catalytic activity, Y· content by whole-cell EPR, and protein concentrations has also been carried out. The very low concentration of Y· and RNR activity measured in the *rnr4*Δ strain and the ability to generate very low levels of activity and Y· of $^{His}\beta_2$ *in vitro* explains the phenotypic consequences of *RNR4* deletion. These *in vitro* and *in vivo* results support the hypothesis that the $\beta\beta'$ is the active form of yeast R2 *in vivo*.

## MATERIALS AND METHODS

*Materials.* Talon resin was obtained from BD Biosciences. Complete protease inhibitor tablets, calf intestine alkaline phosphatase, and DNaseI from bovine pancreas were obtained from Roche. Biotinylated thrombin and Streptavidin agarose were obtained from Novagen. Spin filter microcentrifuge tubes, with a 0.45 μM cellulose acetate filter, were obtained from Corning. Amicon ultra YM30 centrifugal devices were purchased from Millipore. Bradford reagent, anti-MYC, anti-HA, anti-FLAG agarose, 3×FLAG peptide (consisting of three tandem copies of the FLAG epitope), HA peptide, and all other chemicals were obtained from Sigma−Aldrich.

*Protein Purification.* Purification of α, $^{His}\beta_2$, and $\beta'_2$, *in vitro* reconstitution of the diferric-Y· cofactor, RNR nucleotide reduction assay, and ferrozine assay to determine iron content were carried out as described (*7*, *9*). The concentration of $^{His}\beta_2$, $\beta'_2$, and the $^{His}\beta\beta'$ were determined using the known extinction coefficients ($\epsilon_{280-310}$) 105 600, 94 000, and 99 800 $M^{-1}$ $cm^{-1}$, respectively (*7*). The protein concentration for α, α′, and crude extracts were determined by the Bradford assay, with BSA as the standard.

*Vector Construction for Expression of $^{HA}\beta'_2$ in E. coli and Its Purification.* The plasmid for expression of $\beta'_2$ fused to an N-terminal HA tag ($^{HA}\beta'_2$) in *E. coli*, pMH784, was constructed as follows. The 2.75-kb *Nhe* I−*Arv* II genomic DNA fragment containing *RNR4* was subcloned into the *Xba* I site of pRS413 (*16*), resulting in pMH131. An *Nde* I site was created at the first ATG of *RNR4* by site-directed mutagenesis of pMH131 to generate pMH164. pMH164 was digested with *Nde* I and *Xho* I, and the resulting 1.2-kb fragment containing *RNR4* was ligated into the *Nde* I and *Xho* I sites of pETxHA (*17*) to generate pMH784. pMH784 was transformed into BL21(DE3) CodonPlus RIL cells with selection on LB/ampicillin. $^{HA}\beta'_2$ was expressed and purified as described previously for $\beta'_2$ (*9*). A typical recovery was 75 mg of $^{HA}\beta'_2$ from 4.5 g of cell paste.

*Differential Scanning Calorimetry (DSC).* Stock solutions of $^{His}\beta_2$ (84 μM) and $\beta'_2$ (110 μM) were diluted with 50 mM HEPES (pH 7.6), 100 mM NaCl, and 5% glycerol (DSC buffer) to final concentrations of 5.2 μM for $^{His}\beta_2$ and 1.5 μM for $\beta'_2$. Apo-$^{His}\beta\beta'$ (40 μM) was exchanged into DSC buffer by dialysis overnight at 4 °C (Slide-a-lyzer, 30-kDa MWCO, Pierce). The dialyzed $^{His}\beta\beta'$ was then diluted in DSC buffer to a final concentration of 4.2 μM. All buffer and protein solutions were passed through a 0.2 μm filter and degassed for 5 min using a ThermoVac at 10 °C, while stirring with a small magnetic stir bar. The DSC experiments

were performed with a VP-DSC microcalorimeter (Microcal) equipped with a matching sample and reference cells (0.52 mL). Experiments were performed at a scan rate of 90 °C/h for $\beta'_2$ or 60 °C/h for $^{His}\beta_2$ and $^{His}\beta\beta'$. A pre-scan equilibration period of 15 min was applied to allow the temperatures in the sample and reference cells to stabilize. The scans were collected using a passive feedback mode and a filtering period of 16 s for $\beta'_2$ or 8 s for $^{His}\beta_2$ and $^{His}\beta\beta'$. Data were analyzed using the DSC software package from Microcal.

*Rate of Apo-$^{His}\beta\beta'$ Formation from $^{His}\beta_2$ and $\beta'_2$.* $^{His}\beta_2$ was diluted into 25 mM HEPES (pH 7.4), 10% glycerol, 100 mM NaCl, and 1 mg/mL BSA (buffer A) to a final volume of 900 $\mu$L and a concentration of 1.1 $\mu$M. This solution was preincubated at 25 °C for 5 min. The exchange reaction was initiated by the addition of 100 $\mu$L of $\beta'_2$ from a 10 $\mu$M stock in buffer A that had also been pre-equilibrated at 25 °C. The final concentration of $^{His}\beta_2$ and $\beta'_2$ was 1 $\mu$M. Aliquots (75 $\mu$L) were removed and passed through a 100 $\mu$L Talon column. Immediately after the protein solution was soaked into the column (~5 s), the column was washed with 3 mL of buffer A without BSA. The bound protein was eluted with 300 $\mu$L of 300 mM imidazole in buffer A without BSA. The eluted protein was analyzed by 12% SDS−PAGE. Coomassie-stained bands were quantified by comparison to a standard curve of $^{His}\beta$ and $\beta'$ using a ChemiDoc XRS and the QuantityOne software (BioRad).

*Apo-$^{His}\beta\beta'$ Exchange with $^{HA}\beta'_2$.* $^{His}\beta_2$ and $\beta'_2$ were mixed at 25 °C for 15 min to generate the apo-$^{His}\beta\beta'$ at a concentration of 1 $\mu$M in a final volume of 750 $\mu$L of 50 mM HEPES (pH 7.4), 50 mM KCl, 100 mM NaCl, and 10% glycerol (buffer B). The exchange reaction was initiated by the addition of $^{HA}\beta'_2$ to a final concentration of 0.5 $\mu$M from a concentrated stock solution also preincubated at 25 °C. Aliquots (120 $\mu$L) were removed and incubated with 25 $\mu$L of Talon resin in a spin filter tube with gentle mixing for 1 min. The unbound protein was removed by centrifugation at room temperature at 700*g* for 2 min, and the column was washed with 3 mL of buffer B in six 500 $\mu$L aliquots. The bound protein was eluted from the resin with 60 $\mu$L of 25 mM HEPES (pH 7.4), 25 mM KCl, 50 mM NaCl, 500 mM imidazole, and 5% (v/v) glycerol and analyzed on a 12% SDS−PAGE gel.

*Thrombin Cleavage of the His Tag from Holo-$^{His}\beta\beta'$.* Holo-$^{His}\beta\beta'$ (3.4 mg) was mixed with 3 units of biotinylated thrombin for 1 h on ice in 50 mM HEPES (pH 7.4) and 5% glycerol. The holo-$^{His}\beta\beta'$ has a specific activity of 2000 nmol min$^{-1}$ mg$^{-1}$, 0.3 Y•/$^{His}\beta\beta'$ and 1.3 irons/$^{His}\beta\beta'$. The thrombin was removed by incubation with Streptavidin agarose (250 $\mu$L of agarose slurry in storage buffer as supplied by the manufacturer) for 30 min on ice with periodic gentle mixing. The mixture was transferred to a spin filter microcentrifuge tube, and the resin-bound protease was separated from the $\beta\beta'$ by centrifugation at 700*g*. The $\beta\beta'$ was incubated with 250 $\mu$L of Talon resin to remove the cleaved His tag and any remaining $^{His}\beta\beta'$. The mixture was transferred to a spin filter tube, and the Talon resin was removed. RNR activity assay of the thrombin-cleaved heterodimer revealed that removal of the His tag did not change its specific activity.

*Holo-$\beta\beta'$ Exchange with $^{His}\beta_2$.* $^{His}\beta_2$ and holo-$\beta\beta'$ were mixed in buffer B at a final concentration of 1 $\mu$M and a final volume of 14 mL. A control reaction was carried out in parallel, which was treated exactly the same as the exchange experiment except that $^{His}\beta_2$ was omitted. This control allowed for correction for the loss of iron, radical, and activity associated with protein loss during the extensive washing and concentration steps in the experiment. The exchange reaction was incubated at 25 °C for 2 h, and the entire mixture was passed through a 750 $\mu$L Talon column. The flow through (FT) and the first 2 mL of the wash were collected and concentrated to less than 500 $\mu$L with an Amicon ultra YM30 centrifugal device. The column was washed with an additional 4 mL of buffer B, and the bound protein was eluted with 4 mL of buffer B with 200 mM imidazole. The eluted protein was concentrated to less than 500 $\mu$L with an Amicon ultra YM30 concentrator. The concentration of radical was determined by EPR as outlined below for whole-cell EPR experiments. The RNR activity was determined using the standard yeast RNR activity assay utilizing $\alpha$ with a specific activity of 200 nmol min$^{-1}$ mg$^{-1}$ (*7*).

*Yeast Strains and Plasmids.* The yeast plasmid pMH176 for expression of the galactose inducible 3× Myc-tagged $\beta'$ ($^{Myc}\beta'$) was provided by Prof. S. J. Elledge (Harvard Medical School) (*6*).

MHY343 (*MATx*, *can1-100*, *ade2-1*, *his3-11,14*, *leu2-3*, *trp1-1*, *ura3-1*, *rnr2::FLAG-RNR2-Kan*) contains an N-terminally FLAG-tagged $\beta$ ($^{Flag}\beta$) integrated into the endogenous *RNR2* locus. The $^{Flag}\beta$ has the protein sequence MDYKDDDDKH-$\beta$. The construction of pMH725, which was used for integration of *FLAG-RNR2* into the endogenous *RNR2* locus, was complicated, and thus, instead of describing the multiple steps involved in its construction, we will describe the segments in linear order. The backbone of pMH725 is essentially identical to pFA6a-kanMX6 (*18*), except that both the *Nde* I and the *Nco* I sites were removed by digestion with the respective restriction enzyme, treatment with T4 DNA polymerase to fill in the ends, and religation, thus adding six nucleotides to the resulted product, pMH706. Nucleotides 1−1520 in pMH725 are the kanMX6 cassette (*18*). Nucleotides 1521−2971 are the following sequences on the complementary strand: RNR2 promoter sequence, the start codon, and a FLAG-encoding sequence (CC ATG GAC TAC AAA GAC GAT GAC GAC AAT), followed by a *Nde* I site and the coding sequence for the N-terminal 199 residues of $\beta$. The rest of pMH725 (nucleotide 2972−5378) is identical to that of pFA6a-kanMX6 (1534−3938) except for the filled-in *Nde* I site.

MHY343 was generated by integration of a linearized pMH725, which was cut by *EcoR* V in the *RNR2* coding sequence (between codons 118 and 119), into the chromosomal *RNR2* locus. This integration resulted in a *FLAG-RNR2*, under the control of the *RNR2* promoter, as the only full-length *RNR2*-encoding sequence at the endogenous *RNR2* locus. The integration event in MHY343 was confirmed both by PCR analysis of the *RNR2* locus and Western blotting of the expected $^{Flag}\beta$ using both anti-$\beta$ and anti-FLAG Abs.

MHY614 (*MAT**a***, *his3-11,14*, *leu2-3*, *ura3-1*, *rnr4::LEU2*, *rnr2::FLAG-RNR2-Kan*) contains *FLAG-RNR2* integrated into the endogenous *RNR2* locus and deletion of *RNR4*. A *rnr4::LEU2* deletion allele was generated in the diploid strain CUY546 (*5*) by homologous replacement using a 5.4-kb *Nhe* I−*Xho* I fragment as described previously (*6*), resulting in MHY49. A *FLAG-RNR2-kanMX6* was then generated in

MHY49 by integration using a linearized pMH725. The resulting diploid strain, containing both *RNR4/rnr4::LEU2* and *RNR2/FLAG-RNR2-kanMX6*, was sporulated, and a haploid of *rnr4::LEU2, FLAG-RNR2* genotype was isolated by tetrad dissection and confirmation of the *LEU2* and *kanMX6* markers.

MHY346 (*MAT**a**, can1-100, ade2-1, his3-11,14, leu2-3, trp1-1, ura3-1, rnr4::HA-RNR4-Kan*) contains *HA-RNR4* integrated into the endogenous *RNR4* locus. The $^{HA}\beta'$ has the protein sequence: MPYPYDVPDYASLGGH-$\beta'$. pMH708, which was used for integration of *HA-RNR4* into the endogenous *RNR4* locus, was generated by cloning a 2.5-kb *EcoR* I fragment that contains the *RNR4* promoter, the start codon, a HA-encoding sequence, plus a linker sequence (ATG CCT TAC CCA TAC GAT GTT CCA GAT TAC GCT AGC TTG GGT GGT), followed by an *Nde* I site and the coding sequence for the N-terminal 303 residues of $\beta'$. MHY346 was generated by integration of a linearized pMH708, which was cut by *Msc* I in the *RNR4* coding sequence (between codons 211 and 212), into the chromosomal *RNR4* locus. This integration resulted in a *HA-RNR4*, under the control of the *RNR4* promoter, as the only full-length *RNR4*-encoding sequence at the endogenous *RNR4* locus. The integration event in MHY346 was confirmed both by PCR analysis of the *RNR4* locus and Western blotting of the expected $^{HA}\beta'$ using both anti-HA and anti-$\beta'$ Abs.

The wt strain BY4741 (*MAT**a** his3*Δ*1 leu2*Δ*0 met15*Δ*0 ura3*Δ*0*) and *rnr4*Δ strain (isogenic to BY4741 except for *rnr4::KAN*) were obtained from Open Biosystems (*4*).

*In Vivo Concentration of Y*• *by Whole-Cell EPR Spectroscopy*. Yeast cultures (1 L) were grown to mid-log phase ($2 \times 10^7$ cells/mL) in YPD at 30 °C. The doubling times were 90 and 180 min for the wt and *rnr4*Δ strains, respectively. The cells were collected by centrifugation at 7500*g* for 15 min. The cell pellet was washed 2 times with 1 L of ice-cold phosphate-buffered saline (PBS). The pellet was then resuspended in PBS with 30% glycerol to a final concentration of $1-3 \times 10^{10}$ cells/mL. The concentration of cells in the sample was determined by cell counting using a hemacytometer. For each sample, three independent dilutions were made and the average was used as the cell concentration for the data analysis. The standard deviation was typically 15−20%. The cell suspension was transferred to an EPR tube and frozen in liquid nitrogen.

EPR spectra were recorded using a Bruker ESP-300 X-band (9.4 GHz) spectrometer equipped with an internal frequency counter and an Oxford ESR900 liquid helium cryostat to maintain the temperature at 30 K for all samples. Typical instrument parameters were centerfield, 3340 G; sweep width, 100 G; resolution, 2048 points; frequency, 9.38 GHz; modulation amplitude, 2.0 G; conversion time, 81.920 ms; time constant, 40.960 ms; sweep time, 167.772 s; gain, $0.2-5 \times 10^5$; scans, 3−30; and power, 200 or 2.5 $\mu$W for the yeast and *E. coli* Y•, respectively. The double-integral values of the derivative spectra were corrected for differences in power, receiver gain, and number of scans and compared to a standard curve. The Y• of *E. coli* R2 (2.5−115 $\mu$M) was used to generate a standard curve. The concentration of Y• in the *E. coli* standard was determined by the drop-line correction method (*19*), and the protein concentration was determined using the known $\epsilon_{280}$ of 131 $mM^{-1}$ $cm^{-1}$. For determination of the Y• concentration *in vivo*, the EPR spectrum of yeast cells treated with hydroxyurea (150 mM, 1 h) was subtracted from that of untreated cells to subtract contributions from species other than the Y• of RNR as described (*20*). The cell volume used for BY4741 and *rnr4*Δ strains was 41 and 68 fL, respectively (*21*).

*Expression and Purification of $^{Myc}$Y4 from the rnr4*Δ *Strain.* The plasmid pMH176 was transformed into the *rnr4*Δ strain using a standard protocol (*22*). The transformants were selected on Synthetic Complete medium without uracil (SC-Ura). The resulting *rnr4*Δ strain was grown at 30 °C in 2 L of SC-Ura medium with 2% raffinose as the carbon source until the culture reached mid-log phase ($\sim 2 \times 10^7$ cells/mL). The production of $^{Myc}\beta'_2$ was induced with the addition of galactose to a final concentration of 2%, and the cells were grown for an additional 5 h at 30 °C. Cells were collected by centrifugation (7500*g*, 15 min), washed with 50 mL of PBS containing 30% glycerol, and stored at −80 °C.

Cells (6.5 g) were resuspended in 20 mL of 50 mM HEPES (pH 7.4), 1 mM EDTA, 100 mM NaCl, and 10% glycerol (buffer C) supplemented with 25 $\mu$g/mL aprotinin, 10 $\mu$M (2*S*,3*S*)-3-(*N*-{(*S*)-1-[*N*-(4-guanidinobutyl)carbamoyl]3-methylbutyl}carbamoyl)oxirane-2-carboxylic acid (E-64), 0.4 mM 4-(2-aminoethyl)benzenesulfonyl fluoride (AEB-SF), 100 $\mu$g/mL of pepstatin, 100 $\mu$g/mL leupeptin, 100 $\mu$g/mL chymostatin, 1 mM benzamidine, and 50 units of DNaseI. All purification steps were carried out at 4 °C. Cells were lysed by two passes through the French press at 14 000 psi, and cell debris was removed by centrifugation (30000*g*, 30 min). The supernatant was passed through a column (1.5 mL) of anti-Myc agarose 2 times at a flow rate of 0.1−0.2 mL/min. The column was washed with 15 mL of buffer C supplemented with the Complete protease inhibitor tablet. The protein was eluted from the column by the addition of 5 mL of 100 mM ammonium hydroxide. The eluted protein was collected in 1 mL aliquots, and a part of each aliquot was analyzed on a gradient gel (5−15%, BioRad) and stained with the Silver Stain Plus kit, according to instructions of the manufacturer (BioRad). The identity $\beta$ and $^{Myc}\beta'$ was confirmed by Western blotting utilizing $\beta$- or $\beta'$-specific polyclonal Abs.

*Purification of $^{Flag}\beta$ and $^{HA}\beta'$*. The yeast strains MHY343 and MHY346, harboring $^{Flag}\beta$ and $^{HA}\beta'$, respectively, were grown to mid-log phase in YPD (2 L) at 30 °C. These strains grew with a doubling time similar to that for wt cells. Cells were collected by centrifugation (7500*g*, 15 min), washed with 50−100 mL of PBS with 30% glycerol, and stored at −80 °C.

The protein purification was performed at 4 °C. The cell pellets (1−2 g) were resuspended in buffer C supplemented with protease inhibitors as described for the purification of $^{Myc}\beta'_2$. For every gram of cell paste, 10 mL of buffer C was used and 5 units of DNaseI was added for every milliliter of cell suspension. Cells were lysed by two passes through the French press at 14 000 psi. Cell debris was removed by centrifugation (30000*g*, 45 min). The crude supernatant was passed through 500 $\mu$L of either anti-HA or anti-FLAG agarose. Each column was washed with 75 mL of buffer C supplemented with a Complete protease inhibitor tablet. The protein was eluted with the 3×FLAG peptide (100 $\mu$g/mL in buffer C) or the HA peptide (250 $\mu$g/mL in buffer C). Eluted protein was concentrated with an Amicon ultra YM30

centrifugation device. Protein was analyzed on a 12% SDS−PAGE gel and stained with Coomassie. Protein identity was confirmed by Western blotting with $\beta$ or $\beta'$ Abs (*9*).

For purification of $^{Flag}\beta_2$ from the *rnr4*Δ strain, MYH614 was grown in 10 L YPD at 25 °C and had a doubling time of 8−9 h. $^{Flag}\beta_2$ was isolated as described above with a yield of 1 mg from 10 g of cell paste. This protein contained a significant amount of DNA contamination with a $\lambda_{max}$ of 269, and therefore, the protein concentration was determined by a Bradford assay using $^{His}\beta\beta'$ as a standard.

*Yeast Extract Activity Assays.* A yeast culture (2 L) was grown at 30 °C to mid-log phase (1−3 $\times 10^7$ cells/mL) in YPD. The cells were collected by centrifugation at 7500*g* for 15 min. If the activity assay was not performed on the same day as the cell growth, the cell pellet was washed with 50−100 mL of ice-cold PBS with 30% glycerol and stored at −80 °C.

All steps were carried out at 4 °C. The cell pellet (1 g) was resuspended with 10 mL of 50 mM TRIS (pH 7.9), 5% glycerol, 10 mM $MgCl_2$, 300 mM $(NH_4)_2SO_4$, 1 mM EDTA, 1 mM DTT, 25 $\mu$g/mL aprotinin, 10 $\mu$M E-64, 0.4 mM AEBSF, 100 $\mu$g/mL of pepstatin, 100 $\mu$g/mL leupeptin, 100 $\mu$g/mL chymostatin, 1 mM benzamidine, 10 mM NaF, and 100 mM $\beta$-glycerophosphate (buffer D). Cells were lysed by three passes through the French press (14 000 psi), and cell debris was removed by centrifugation (30000*g*, 30 min). DNA was removed by the dropwise addition of polyethylenimine (2% stock solution adjusted to neutral pH) to a final concentration of 0.2%. The precipitate was removed by centrifugation (30000*g*, 30 min). The supernatant was treated with solid ammonium sulfate to 65% saturation (430 mg/mL). The precipitated proteins were collected by centrifugation (30000*g*, 30 min). The protein pellet was dissolved in a minimal volume of buffer D, and 3 mL of the protein was desalted with a Sephadex G-50 column (0.7 × 16 cm) equilibrated in 25 mM HEPES (pH 7.2), 25 mM $MgSO_4$, and 50 mM $(NH_4)_2SO_4$ supplemented with the Complete protease inhibitor tablet. The protein concentration was determined by the Bradford assay and immediately used in an activity assay without freezing. Freezing and storage at −80 °C was found to decrease the activity.

All assays were carried out on extracts partially purified as described above. The assays contained 2−5 mg/mL extract, 30 mM DTT, 3 mM ATP, 1 mM [$^{14}$C]-CDP (5000 cpm/nmol), 100 mM HEPES (pH 7.2), 10 mM $MgSO_4$, and 10 mM NaF. All components except extract were mixed and preincubated at 30 °C for 5 min. The assay was initiated by the addition of extract that was also equilibrated to 30 °C. Aliquots (30 $\mu$L) were removed over 30 min and quenched in a boiling water bath for 2 min. After the pH was adjusted to 8.5 by the addition of 50 $\mu$L of 1 M TRIS (pH 8.5), alkaline phosphatase (60 units) and deoxycytidine (0.5 $\mu$mol) were added and the mixture was incubated at 37 °C for 3 h. The products were analyzed by the method of Steeper and Steuart (*23*).

*Western Blotting.* Typically an aliquot of crude extract (100−500 $\mu$L, before the precipitation of DNA) was removed from the sample generated for activity assays as described above. A portion of this aliquot was utilized to determine the protein concentration by a Bradford assay. The crude extract was diluted into 4× Laemmli (1 part Laemmli/3 parts crude extract), frozen in liquid nitrogen, and stored at −80 °C. Western blots used RNR subunits ($^{His}\alpha$, $^{His}\beta_2$, $\alpha'$, or $\beta'_2$) purified from *E. coli* as standards (*7*, *9*). The standards (2−100 ng) and crude extract (1−10 $\mu$g) were analyzed on a 10% SDS−PAGE gel (BioRad Criterion Gel). The proteins were transferred to PVDF (Sequiblot PVDF, BioRad) using a tank transfer unit in transfer buffer (25 mM TRIS, 192 mM glycine, 10% methanol, and 0.1% SDS at 4 °C) at 56 V for 90 min. Western blots were carried out as described previously, except that the blots were developed with the DuraWest Chemiluminescent Reagent (Pierce) (*7*). The chemiluminescent signal was detected with a CCD camera (ChemiDoc XRS, BioRad). Bands were quantified using BioRad's QuantityOne software. The results of the quantitative Westerns are presented as the concentration of polypeptide *in vivo* and thus are based on monomer molecular weights.

*Co-immunoprecipitation of $\beta$ from rnr4*Δ *Extracts with $^{HA}\beta'_2$.* The wt and *rnr4*Δ strains were grown in YPD at 30 °C to 2 × $10^7$ cells/mL. All steps were performed at 4 °C. The cell pellet (1 g) was resuspended with buffer C supplemented with protease and phosphatase inhibitors as described above, and cells were lysed by 3 passages through the French press at 14 000 psi. Cell debris was removed by centrifugation at 30000*g* for 30 min. The concentration of protein in the extract was determined by the Bradford assay, with BSA as the standard.

Crude extract (0.17−5.4 mg) was mixed with 8 $\mu$g (200 pmol) of $^{HA}\beta'_2$ in buffer B, and the mixture was incubated on ice for 30 min. Anti-HA agarose (20 $\mu$L of agarose beads in a total volume of 40 $\mu$L) was added, and the mixture was incubated for an additional 45 min on ice with periodic mixing. The resin was collected by centrifugation at 700*g* for 5 min and 4 °C. The resin was washed 2 times with 500 $\mu$L of buffer B. The resin was transferred to a spin filter tube, where it was washed with an additional three aliquots (500 $\mu$L) of buffer B. The protein was eluted with 60 $\mu$L of a low-pH IgG elution buffer (Pierce), diluted with 4× Laemmli, and analyzed by SDS−PAGE (12%).

*Assembly of the Diferric-Y• Cofactor from $^{His}\beta_2$, $Fe^{2+}$, and $O_2$.* The reconstitution procedure was followed as described previously with minor changes (*7*, *9*). A stock solution of $^{His}\beta_2$ (4 mg/mL, 42 $\mu$M) in 50 mM HEPES (pH 7.4) and 25% (w/v) glycerol was deoxygenated by repeated cycles of vacuum pumping and argon flushing on a Schlenk line and brought into the anaerobic wet box. A total of 5 equiv of $Fe^{II}/^{His}\beta_2$ were added from a 1 mM deoxygenated $FeSO_4$ solution to the $^{His}\beta_2$ along with sufficient buffer to dilute the protein 2-fold from its initial concentration and incubated at room temperature for 30 min. The protein was removed from the box, and ~$^1/_3$ volume of $O_2$-saturated 50 mM HEPES (pH 7.4), 5% (v/v) glycerol, and 15 mM $MgCl_2$ buffer (buffer D) was added dropwise. Excess iron was removed by applying the mixture to a 10 mL Talon column and washing with 50 mL of buffer D. The protein was then eluted from the column with 20 mL of buffer D plus 200 mM imidazole. Fractions were collected, and those containing protein were pooled and concentrated using an Amicon Centricon fit with a YM30 membrane. The imidazole was removed by passage of the protein over a Sephadex G-25 column previously equilibrated in buffer D. Protein quantification, EPR analysis, and activity assays were carried out as described above.

## RESULTS

*Stability of* $^{His}\beta_2$. Our circular dichroism (CD) and crystallographic studies revealed that $^{His}\beta_2$ (with N-terminal sequence MGSSHHHHHHSSGLVPRGSHM-$\beta$) expressed in and isolated from *E. coli* is a soluble and folded protein (*9*, *13*). Thelander and co-workers have reported that their $^{His}\beta_2$ construct (with N-terminal sequence MHHHHHHM-$\beta$) was unable to fold correctly in *E. coli* as evidenced by inclusion body formation and low recoveries in attempted purifications (*8*). We believe the differences in $^{His}\beta_2$ behavior may be associated with the differences in the His-tag constructs.

The stability of our $^{His}\beta_2$ construct was further examined by a variety of methods, given its difference in behavior relative to the similar construct reported by Chabes et al. Previously, we have shown that the CD spectrum of $^{His}\beta_2$ is similar to that of $\beta'_2$ and that it is a predominantly helical protein (*7*). Removal of the His tag from $^{His}\beta_2$ using thrombin, however, resulted in a large decrease in helical content, indicated by a 30% change in the $\Theta$ at 208 nm (data not shown). Efforts to assemble the diferric-Y$\cdot$ cofactor from the resulting $\beta_2$ and $\beta'_2$, generated $\beta\beta'$ with only 30−40% of the activity routinely obtained with a similar experiment using $^{His}\beta_2$. Finally, we have also observed that when chromatographed on either DEAE- or Q-Sepharose both tagged and untagged $\beta_2$ elute in broad peaks and with low recoveries. These observations together indicate that, while our $^{His}\beta_2$ is soluble and folded, it is unstable.

These findings are perhaps not surprising because, in general, apo-R2s, even *E. coli* R2, are considerably less stable than their cofactor-assembled counterparts. In an effort to quantify the relative stability of the $^{His}\beta_2$ and $\beta'_2$ and the apo-$^{His}\beta\beta'$, each protein was examined using DSC. The results of a typical set of experiments for $^{His}\beta_2$ and $\beta'_2$ are shown in Figure 1. In each case, the unfolding of the protein was followed by irreversible aggregation as indicated by a rapid decline in heat capacity at temperatures $\geq$55 °C for $^{His}\beta_2$ and apo-$^{His}\beta\beta'$ and $\geq$75 °C for $\beta'_2$. This irreversible aggregation prevents extraction of meaningful quantitative data from these melting curves. However, qualitatively, the $T_m$ values (the temperature at the peak of the unfolding curve) measured under similar conditions reflect the relative stabilities of $^{His}\beta_2$, $\beta'_2$, and apo-$^{His}\beta\beta'$. Apo-$^{His}\beta_2$ has a $T_m$ of ~30 °C as compared to 50 °C for $\beta'_2$. The unfolding of apo-$^{His}\beta\beta'$ was immediately followed by a large decrease in the heat capacity associated with precipitation, preventing a reliable determination of the $T_m$ (data not shown). These observations suggest that $\beta_2$ might belong to a growing class of proteins that are partially unfolded *in vivo* (*24*). Alternately, $\beta_2$ could be stabilized *in vivo* through binding to $\beta'_2$ or folding chaperones.

*Rate of Exchange of* $^{His}\beta_2$ *with* $\beta'_2$ *To Form Apo-*$^{His}\beta\beta'$ *Is Fast.* We have shown that apo-$^{His}\beta\beta'$ can be reconstituted from $^{His}\beta_2$ and $\beta'_2$ expressed and purified independently (*7*). However, it is important to measure the kinetics of this reorganization as an indicator of whether this process could occur under physiological conditions. Furthermore, Chabes et al. reported that, when $^{His}\beta_2$ and $\beta'_2$ were mixed for 10 min at 30 °C in the presence of $Fe^{2+}$, DTT, and $O_2$, this mixture had only 2% of the activity observed with their $^{His}\beta\beta'$ isolated from coexpression of *HIS*−*RNR2* and *RNR4*. They concluded from these observations that $\beta$ and $\beta'$ must to be cotranslated to efficiently form $\beta\beta'$ or that other cellular components are required (*8*). To measure the rate of $\beta\beta'$ formation, $^{His}\beta_2$ and $\beta'_2$ were mixed at concentrations found *in vivo* (1 $\mu$M) (*7*). Aliquots were removed from this mixture over 5 min and quickly passed through columns containing the Talon resin, which efficiently binds the His tag in either $^{His}\beta_2$ or $^{His}\beta\beta'$. Control experiments were carried out to ensure that the binding capacity of the resin was sufficient to quantitatively bind the $^{His}\beta$. After the column was washed to remove any $\beta'_2$ that had not exchanged to generate $^{His}\beta\beta'$, the bound protein was eluted with imidazole and the products of exchange were analyzed by SDS−PAGE ($^{His}\beta$, 48 kDa; $\beta'$, 40 kDa; Figure 2). To quantify the extent of exchange, the ratio of $^{His}\beta/\beta'$ at each time point was analyzed by densitometry. Apo-$^{His}\beta\beta'$ forms rapidly because a band for $\beta'$ can be seen within 10 s of mixing $^{His}\beta_2$ and $\beta'_2$. Apo-$^{His}\beta\beta'$ formation is complete within 2 min, demonstrating that its rate of formation is sufficiently fast to be physiologically relevant. However, one should remember that the $\beta_2$ used in these experiments is modified by a His tag.

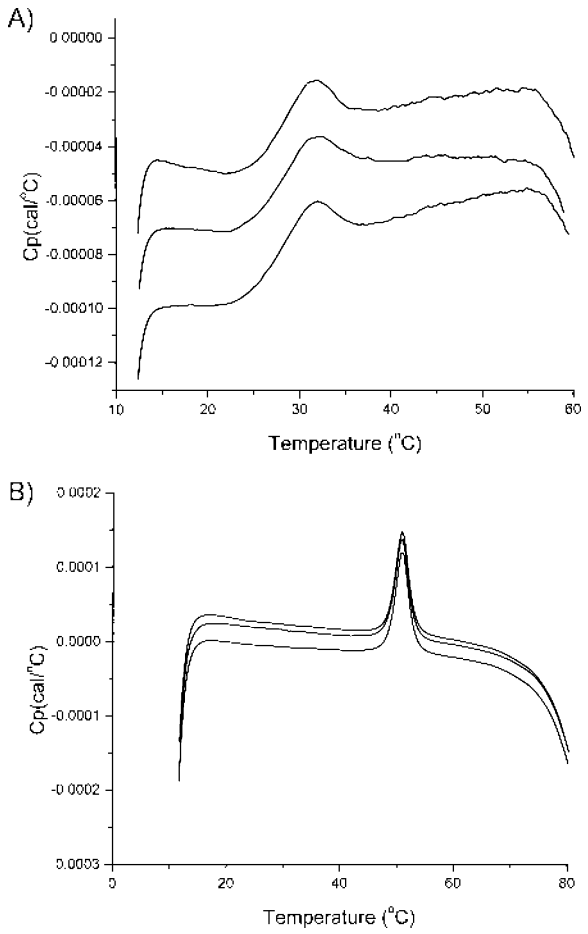


FIGURE 1: DSC experiments with $^{His}\beta_2$ and $\beta'_2$. (A) Thermal denaturation curves of 5.2 $\mu$M $^{His}\beta_2$. Three scans were acquired under identical conditions as described in the Materials and Methods. (B) Thermal denaturation curves of 1.5 $\mu$M $\beta'_2$. Three scans were acquired under identical conditions as described in the Materials and Methods.

*Exchange of Apo-*$^{His}\beta\beta'$ *with* $^{HA}\beta'_2$ *To Form Apo-*$^{His}\beta^{HA}\beta'$. An exchange reaction was carried out to test the ability of apo-$^{His}\beta\beta'$ to undergo further exchange (Figure 3). $^{His}\beta_2$ and $\beta'_2$ were mixed at a final concentration of 1 $\mu$M and allowed to equilibrate to form apo-$^{His}\beta\beta'$. An aliquot was removed from this mixture, passed through a metal-affinity resin and

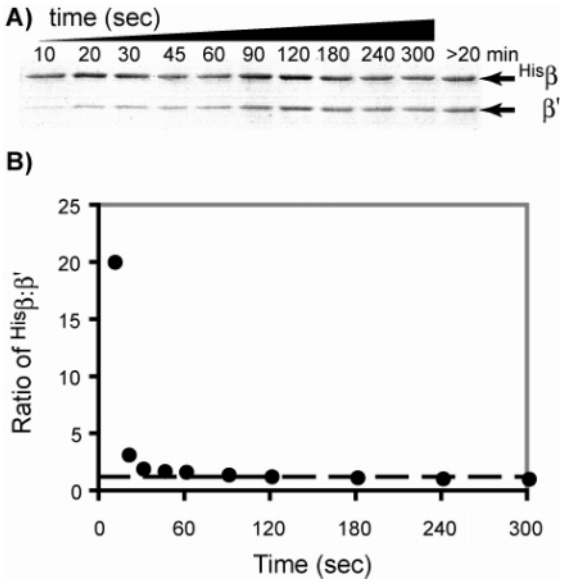


FIGURE 2: SDS−PAGE and densitometry analysis of the rate of $\beta\beta'$ formation. (A) SDS−PAGE (12%) analysis of the metal-affinity column-bound fraction. $^{His}\beta_2$ and $\beta'_2$ were mixed at a final concentration of 1 $\mu$M and incubated at 25 °C. At the times indicated above each lane, an aliquot was removed and subjected to metal-affinity chromatography. The bound protein consisting of $^{His}\beta_2$ and/or $^{His}\beta\beta'$ was eluted with imidazole and analyzed by SDS−PAGE. (B) Densitometry analysis of the SDS−PAGE gel shown in A. The intensity of each protein band was quantified by a comparison to a standard curve generated using known amounts of $^{His}\beta$ or $\beta'$. The ratio of $^{His}\beta/\beta'$ for each lane is plotted as a function of incubation time before separation of the products by metal-affinity chromatography. The dotted line represents the 1:1 ratio of $^{His}\beta/\beta'$.

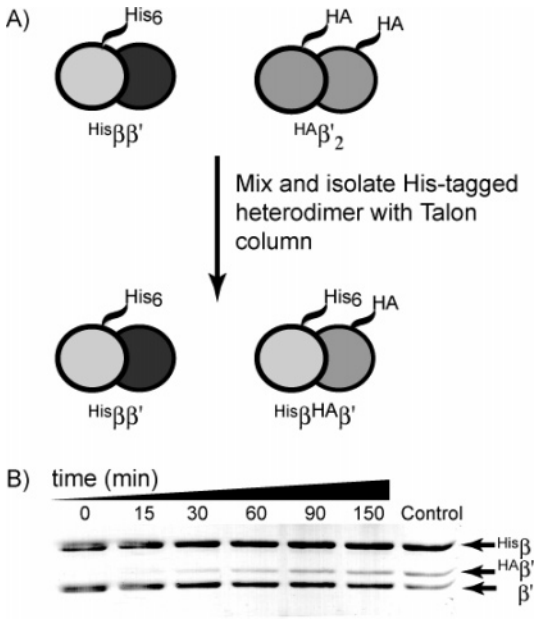


FIGURE 3: Exchange of apo-$^{His}\beta\beta'$ with $^{HA}\beta'_2$. Apo-$^{His}\beta\beta'$ was mixed with the $^{HA}\beta'_2$ and at the times indicated above each lane; an aliquot was removed and subjected to metal-affinity chromatography. The bound protein, containing a mixture of $^{His}\beta\beta'$ that has not undergone any protomer exchange and $^{His}\beta^{HA}\beta'$, was eluted, and the products were analyzed by SDS−PAGE (12%). For the lane marked control, the $^{HA}\beta'_2$ and $\beta'_2$ were mixed before the addition of $^{His}\beta_2$ to generate the heterodimer mixture containing an equal concentration of $^{His}\beta\beta'$ and $^{His}\beta^{HA}\beta'$.

eluted to demonstrate that apo-$^{His}\beta\beta'$ had quantitatively formed (Figure 3B, $t = 0$). $^{HA}\beta'_2$ (1 $\mu$M) was then added to the apo-$^{His}\beta\beta'$, and the mixture was incubated for 2.5 h. Aliquots were removed over this period and subjected to metal-affinity chromatography. After washing and elution of the bound protein, the products of the exchange reaction were analyzed by SDS−PAGE (Figure 3B). A band for $^{HA}\beta'$ can be seen slowly increasing over time, indicating that the apo-$^{His}\beta\beta'$ is capable of undergoing exchange. Interestingly, the rate at which this species exchanges its protomers is much slower than the rate of apo-$^{His}\beta\beta'$ formation. After several hours of incubation, the ratio of $^{HA}\beta'/\beta'$ was only about 1:3. To ensure that the HA tag on $\beta'$ does not affect that stability of the apo-$^{His}\beta^{HA}\beta'$, a control experiment was completed in which $^{HA}\beta'_2$ and $\beta'_2$ were mixed together at equimolar concentrations before the addition of an equimolar amount of $^{His}\beta_2$. If the HA tag does not have an effect on the relative stability of the heterodimer, then the $^{His}\beta\beta'$ and $^{His}\beta^{HA}\beta'$ should be formed in equal amounts. This mixture was passed through a Talon column to isolate any heterodimer that had formed during this control exchange reaction. As seen in the last lane in Figure 3B, the ratio of $^{HA}\beta'/\beta'$ in this isolated heterodimer mixture is 1:1, suggesting that the presence of the HA tag does not affect heterodimer formation. These results demonstrate that protomer exchange is possible from apo-$^{His}\beta\beta'$. However, the slow rate of exchange at physiological concentrations indicates that it is probably not physiologically important.

*Holo-$\beta\beta'$ Does Not Exchange with $^{His}\beta_2$ To Form Holo-$\beta_2$.* We wanted to determine if a cofactor-loaded $\beta_2$ could be generated from apo-$^{His}\beta_2$ and holo-$\beta\beta'$. To differentiate between $\beta$ originating from $^{His}\beta_2$ and the holo-heterodimer (holo-$\beta\beta'$), the His tag was removed from the latter using thrombin. Several problems complicated data analysis from this experiment. The first is that the holo-$\beta\beta'$ used in our experiments contains only 1.3 irons and 0.3 Y· because of our inability to stoichiometrically assemble the cofactor *in vitro*. Therefore, only 30% of the holo-$\beta\beta'$ has a fully assembled diferric-Y· cofactor, and the remaining 70% includes apo-$\beta\beta'$ and partially iron-loaded heterodimer. Thus, some exchange is possible between the apo forms of these proteins. The second problem is associated with the instability of $^{His}\beta_2$ discussed above and the low concentrations used in the exchange reaction (1 $\mu$M) to mimic physiological conditions. Because of these problems, typical protein recoveries are only ~80%. To control in part for the protein loss in this experiment, the holo-$\beta\beta'$ was subjected to the same conditions in the absence of $^{His}\beta_2$.

Three different outcomes are possible in this experiment and are illustrated in Figure 4A, 1−3. Figure 4A1 describes the products expected if the holo-$\beta\beta'$ exchanges only with itself to form holo-$\beta_2$ and $\beta'_2$ but not with $^{His}\beta_2$. All of the iron, radical, and enzymatic activity would be found in the FT of the Talon column. During the purification of holo-$^{His}\beta\beta'$, we previously demonstrated that the ratio of $^{His}\beta/\beta'$ remains 1:1 after metal-affinity and anion-exchange chromatography (*7*). Thus, this possibility is ruled out.

Two additional exchange processes are possible (Figure 4A2 and 3) that would result in different partitioning of the Y· containing $^{His}\beta$ into either the metal-affinity column-bound or FT fractions. If the holo-$\beta\beta'$ exchanges with $^{His}\beta_2$ (Figure 4A2), then the column-bound fraction should contain Y· as a result of the generation of holo-$^{His}\beta\beta$. Alternately, if no exchange occurs between $^{His}\beta_2$ and holo-$\beta\beta'$ (Figure 4A3),

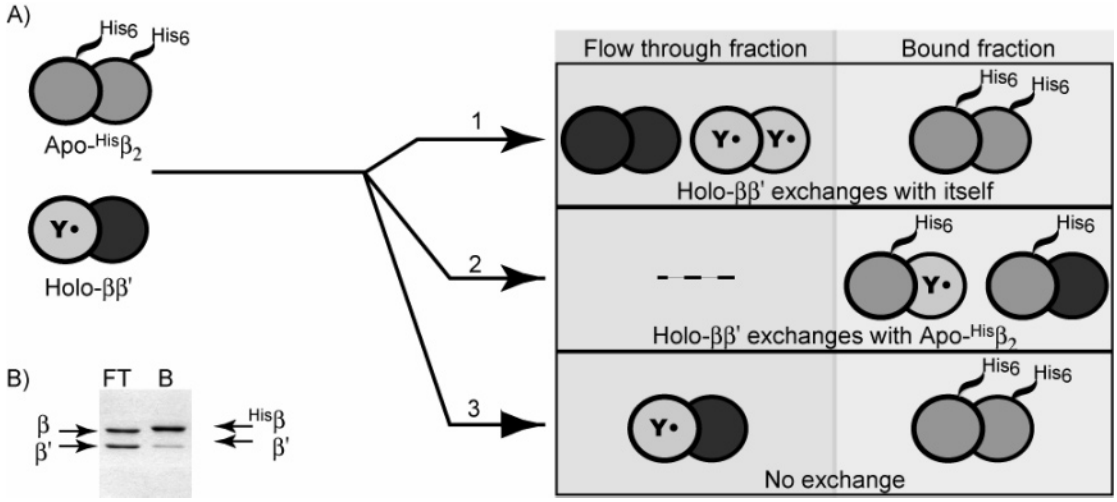


FIGURE 4: Holo-$\beta\beta'$ does not undergo any protomer re-organization. (A) Outline of the exchange experiment and possible outcomes. (1) Holo-$\beta\beta'$ exchanges with itself to generate a holo-$\beta_2$ that would be isolated in the FT fraction; (2) Holo-$\beta\beta'$ exchanges with $^{His}\beta_2$ to generate a holo-$^{His}\beta\beta$, which would be found in the column-bound fraction; and (3) no exchange resulting in isolation of holo-$\beta\beta'$ in the FT fraction and $^{His}\beta_2$ in the bound fraction. (B) SDS−PAGE analysis of the observed products present in the FT and bound (B) fractions.

Table 1: Holo Exchange Experiment[a]

| | flow-through fraction [experiment (control)][b] | bound fraction [experiment (control)] |
|---|---|---|
| activity | 84% (79%) | 1% (ND)[c] |
| iron | 76% (93%) | 24% (19%) |
| radical | 86% (83%) | 1% (ND)[c] |

[a] The percent recovery of the activity, iron, and radical present in the initial 14 nmol of $\beta\beta'$ heterodimer added to the exchange experiment. [b] The control consisted of only the holo-$\beta\beta'$ in the absence of $^{His}\beta_2$ to control for the loss of activity, iron, and radical because of the loss of protein and not an exchange process. [c] ND = none detected.

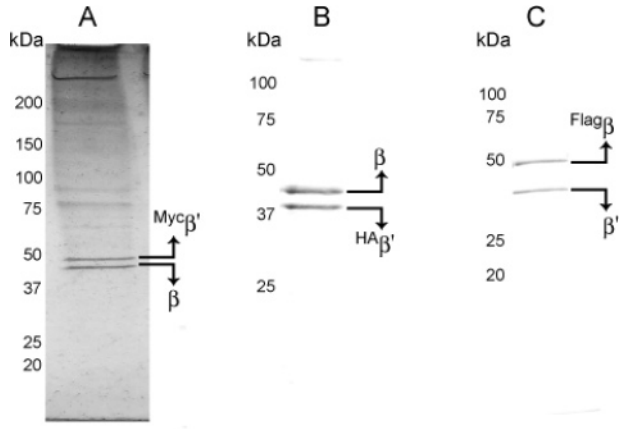


FIGURE 5: Isolation of *S. cerevisiae* R2 using a variety of tagged $\beta$ and $\beta'$ constructs. SDS−PAGE analysis of products purified using antibody-based affinity resin. (A) Anti-Myc agarose was utilized to isolate $^{Myc}\beta'$ overexpressed in the *rnr4*Δ strain. (B) Anti-HA agarose was utilized to isolate $^{HA}\beta'$ from MHY346 crude extracts. (C) Anti-FLAG agarose was utilized to isolate $^{Flag}\beta$ from MHY343 crude extracts.

then all of Y•, iron, and activity should be recovered in the column FT. As shown in Figure 4B and summarized in Table 1, the FT fraction contains 75−85% of the total activity, iron, and Y•, supporting scenario 4A3 in which the diferric-Y• cofactor in $\beta$ prevents subunit exchange.

Analysis revealed that the Talon-bound fraction had a small amount of iron, Y•, and activity above the amounts observed in the control (Table 1). SDS−PAGE analysis revealed that the bound fraction also contained small amounts of $\beta'$ (Figure 4B), suggesting the presence of cofactor holo-$^{His}\beta\beta'$. As noted above, a likely explanation of these observations is our inability to stoichiometrically generate holo-$^{His}\beta\beta'$. The apo-$\beta\beta'$ could slowly exchange with $^{His}\beta_2$ to form apo-$^{His}\beta\beta'$, which could subsequently pick up adventitious iron during the experiment and assemble the small amount of the diferric-Y• cofactor observed in the bound fraction.

It is also possible that this small amount of cofactor associated with the column-bound fraction arose from the exchange process outlined in Figure 4A2. However, less than 1% exchange occurred over 2 h, suggesting that this process is not physiologically important. Thus, cofactor-loaded $\beta_2$ cannot be formed from the heterodimer, suggesting that the active form of the yeast R2 *in vitro* is $\beta\beta'$.

*Isolation of ββ′ from Yeast Crude Cell Extracts.* The experiments presented thus far have been designed to probe the relative stabilities of $^{His}\beta_2$, $\beta'_2$, and $^{His}\beta\beta'$ *in vitro* and have shown that, once iron is loaded into the heterodimer, no further re-organization is observed. The *in vitro* data do not, however, rule out the possibility that this re-organization could occur *in vivo* with the assistance of accessory proteins that have not yet been identified. In fact, the viability of the *rnr4*Δ strain suggests that there must be a mechanism for activation of $\beta_2$ *in vivo*. Thus, a number of experiments utilizing epitope-tagged R2s and gene-deletion strains have been carried out to explore the relative stabilities of the homodimers and heterodimer *in vivo*.

To investigate the active form(s) of yeast R2 *in vivo*, $^{Myc}\beta'$ was overexpressed from a plasmid transformed into the *rnr4*Δ strain. Anti-Myc agarose was used to purify $^{Myc}\beta'$, and a 1:1 complex of $\beta/^{Myc}\beta'$ was isolated (Figure 5A). To ensure that the isolation of the heterodimeric complex was not an artifact because of overexpression of $^{Myc}\beta'$, similar experiments were carried out with two additional yeast strains chosen because the epitope-tagged $\beta$ or $\beta'$ are under control of their native promoters integrated in their respective chromosomal loci and therefore are not overexpressed. The yeast strain MHY346 contains a gene replacement of wt

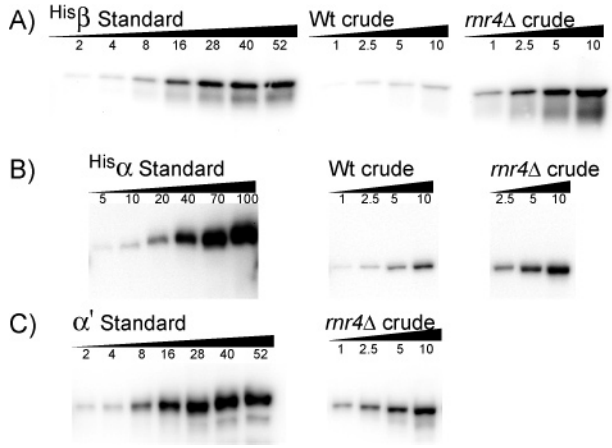


FIGURE 6: Quantitative Western blots to determine the concentration of $\beta$ (A), α (B), and α′ (C) in wt and *rnr4*Δ strains. The nanogram of standard or microgram of crude extract loaded is indicated above each lane.

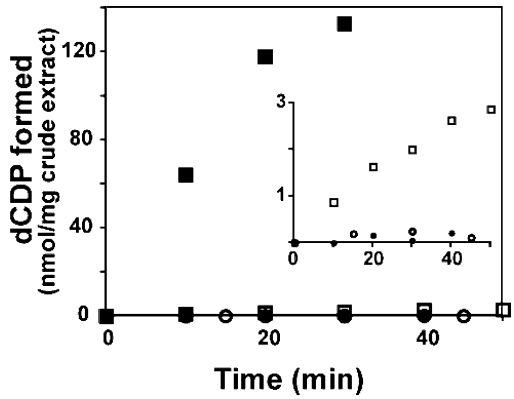


FIGURE 7: Assays of RNR activity in yeast extracts. The total nanomoles of dCDP produced as a function of time are plotted for the wt extract (□), wt extract supplemented with 4 $\mu$M α (■), *rnr4*Δ extract (○), and *rnr4*Δ extract supplemented with 6 $\mu$M α (●). The inset has the same data but on a different scale.

*RNR4* by *HA-RNR4*, which encodes an N-terminally HA-tagged $\beta'$ that has been integrated into the endogenous *RNR4* locus. The $^{HA}\beta'$ was isolated with anti-HA agarose from crude extract generated from MHY346. As shown in Figure 5B, a 1:1 complex of $\beta/^{HA}\beta'$ was isolated. To further confirm these results, the heterodimer was isolated from the yeast strain MHY343, which contains an exact insertion of a FLAG epitope encoding sequence at the 5′ end of the *RNR2* open-reading frame in its chromosomal locus. $^{Flag}\beta$ was purified using an anti-FLAG agarose resin, and again, a 1:1 $^{Flag}\beta/\beta'$ complex was isolated (Figure 5C). These results strongly support our *in vitro* observations that under these growth conditions holo-$\beta\beta'$ does not undergo re-organization to form holo-$\beta_2$ and $\beta'_2$. Our data also strongly support the hypothesis that $\beta\beta'$ is the active form of yeast R2 *in vivo*.

*β′ Plays a Role in Cluster Assembly in Vivo*. Having confirmed the predominant presence of $\beta\beta'$ *in vivo*, we wanted to probe the role of $\beta'$ in generating active yeast R2. Previous studies have shown that *RNR4* is essential for mitotic viability in the W303 strain background (*6*). However, two *RNR4* deletion strains have been constructed with phenotypes of slow growth and cold sensitivity, demonstrating that $\beta_2$ must be active in nucleotide reduction in the absence of $\beta'_2$ (*4*, *5*). Examination of these strains might give us insight about the mechanism of cell survival and specifically the ability of $\beta_2$ to substitute for $\beta\beta'$. Isogenic strains of wt and *rnr4*Δ were examined using quantitative Western blotting, whole-cell EPR spectroscopy, and activity assays to gain a better understanding of the phenotypic consequences of *RNR4* deletion.

RNR subunit concentrations in wt and *rnr4*Δ strains were determined using quantitative Western blotting and are reported herein as the concentrations of protein monomer (α, $\beta$, α′, and $\beta'$). As shown in Figure 6 and Table 2, the RNR subunits, α, $\beta$, and α′, are all overexpressed in the *rnr4*Δ strain. $\beta$ is expressed at a concentration of 0.8 ± 0.3 $\mu$M in this wt strain background. In the otherwise isogenic *rnr4*Δ strain, $\beta$ is present at 14 ± 4 $\mu$M. Therefore, the $\beta$ concentration increases roughly 15-fold upon deletion of *RNR4*. The expression levels of α and α′ are also increased in the *rnr4*Δ strain. The amount of α/cell increases ~2.5-fold, but because the cell volume of the *rnr4*Δ strain is larger than the wt strain, the concentration of α is 0.9 ± 0.3 $\mu$M, similar to that in the wt strain (0.8 ± 0.3 $\mu$M). α′ cannot be detected in wt extracts but is induced to a concentration of 1.8 ± 0.5 $\mu$M in the *rnr4*Δ strain.

The effect of *RNR4* deletion on the RNR activity was measured in cell extracts that have undergone polyethyleneimine and ammonium sulfate fractionation (*25*). Western blotting confirmed that this procedure did not remove α, $\beta$, and $\beta'$. This partial purification is essential for the detection of activity. Cell extracts prepared in this way typically have a specific activity of 0.06 ± 0.01 nmol min$^{-1}$ mg$^{-1}$ (inset of Figure 7). The addition of α (4 $\mu$M) to the extract results in a 60-fold increase in CDP reduction activity to 3.7 nmol min$^{-1}$ mg$^{-1}$, presumably because the endogenous $\beta\beta'$ in the extract is saturated with α under these conditions. On the other hand, no activity was measurable in the *rnr4*Δ extracts, even after α was added to a final concentration of 6 $\mu$M (inset of Figure 7). Thus, the activity in the *rnr4*Δ strain extracts must be less than 0.01 nmol min$^{-1}$ mg$^{-1}$. Even though $\beta$ is overexpressed in the *rnr4*Δ strain relative to the wt strain, the *rnr4*Δ extract has a specific activity that is at least 100-fold less that the activity of the wt extract.

To understand the basis for the dramatic drop in RNR activity, a whole-cell EPR technique was used to measure the concentration of Y· *in vivo*. Harder and Follmann first reported the doublet signal associated with the Y· of *S. cerevisiae* R2 in extracts subjected to an ammonium sulfate fractionation (*26*). They noted that the signal could also be observed in whole cells. Figure 8 shows a comparison of

Table 2: Summary of the Concentrations of the RNR Subunits in the wt and *rnr4*Δ Strains Determined by Quantitative Western Blotting and Y· Concentration Determined by Whole-Cell EPR

| strain | cell volume (fL) | [Y·] ($\mu$M) | [$\beta$] ($\mu$M) | [$\beta'$] ($\mu$M) | [α] ($\mu$M) | [α′] ($\mu$M) |
|---|---|---|---|---|---|---|
| wt (BY4741) | 41 | 0.8 ± 0.2 | 0.8 ± 0.3 | 0.5 ± 0.2 | 0.8 ± 0.3 | <0.03[a] |
| *rnr4*Δ | 68 | <0.05 | 14 ± 4 | | 0.9 ± 0.3 | 1.8 ± 0.5 |

[a] On the basis of the lower limit of detection at 1 ng in 10 $\mu$g of crude extract.

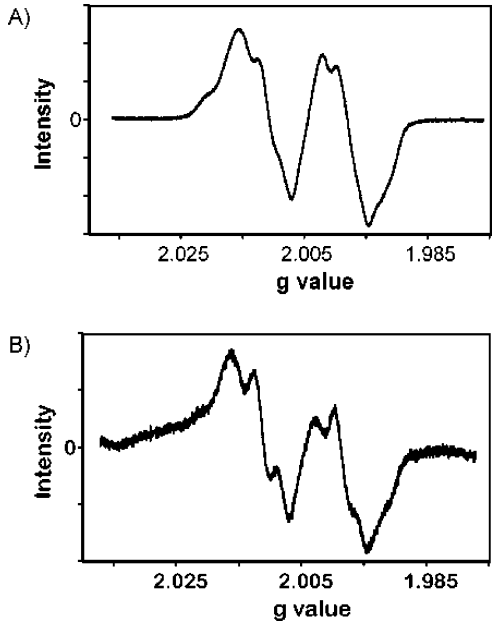


FIGURE 8: EPR spectra of pure $^{His}\beta\beta'$ and whole yeast cells. (A) EPR spectrum of $^{His}\beta\beta'$ (20 $\mu$M, 0.2 Y·/heterodimer) was acquired with 10 scans at a receiver gain of $1 \times 10^5$. All other EPR settings are as described in the Materials and Methods. (B) EPR spectrum of whole yeast cells (BY4741; $1.12 \times 10^{10}$ cells/mL) was acquired with 32 scans at a gain of $1.78 \times 10^5$.

purified $^{His}\beta\beta'$ (A) and the EPR spectrum acquired from wt yeast cells (B). Double integration of this signal and a comparison to a standard curve of *E. coli* R2 Y·, as well as the assumption of a cell volume of 41 fL, allowed determination of the Y· concentration to be $0.8 \pm 0.2$ $\mu$M (*20*). The EPR spectrum acquired from the *rnr4*Δ cells is very different from that of the wt cells. No Y· could be detected above the background signal, and the line shape was reminiscent of the spectra acquired from wt yeast cells treated with hydroxyurea, a chemical that leads to the reduction of the Y· (data not shown). On the basis of our estimation of the lower limit of detection, the Y· concentration in the *rnr4*Δ strain must be at least 20-fold lower than in wt cells even though the $\beta$ concentration is elevated approximately 15-fold. This observation explains why the strain lacking $\beta'$ has a dramatic decrease in RNR activity. These results demonstrate that $\beta'$ plays a crucial role in diferric-Y· assembly in $\beta$ *in vivo*. Furthermore, they demonstrate that the measurement of the RNR protein concentration does not necessarily correlate with RNR activity *in vivo*.

*Re-examination of Diferric-Y· Assembly with* $^{His}\beta_2$ *and* $^{Flag}\beta_2$. The above results indicate that $\beta_2$ must be able to assemble a minimal amount of diferric-Y· cofactor and that this assembled protein must be able to interact with α to effect nucleotide reduction. On the basis of the doubling time of the *rnr4*Δ strain, the concentration of the $\beta$ and the size of the yeast genome, $\beta_2$, must have a minimal specific activity of 5 nmol min$^{-1}$ mg$^{-1}$ to support DNA replication. Thus, we re-examined the Y· content and specific activity of $^{His}\beta_2$, which we previously reported was inactive in nucleotide reduction (*9*), under conditions that would allow for detection of low amounts of Y· and activity. The reconstitution was completed on a larger scale than in previous experiments to give a sufficiently high concentration of $^{His}\beta_2$ for Y· content determination, and the CDP utilized in the nucleotide reduction assay had a high specific activity

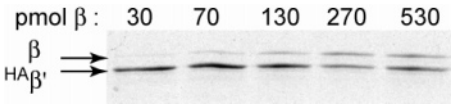


FIGURE 9: SDS−PAGE analysis of co-immunoprecipitation of $^{HA}\beta'$ and $\beta$ from the *rnr4*Δ crude extracts. Crude extract was generated from the *rnr4*Δ strain, and increasing amounts of the extract was mixed with 200 pmol of $^{HA}\beta'$, which was subsequently immunoprecipitated using anti-HA agarose. The total amount of $\beta$ in each immunoprecipitation experiment, estimated from quantitative Western blotting, is indicated above each lane.

(~7000 cpm/nmol) relative to that routinely used for $^{His}\beta\beta'$ assays (~2000 cpm/nmol). After reconstitution by our standard procedures, $^{His}\beta_2$ was assayed for activity and monitored for Y· and was found to have a specific activity of 10 nmol min$^{-1}$ mg$^{-1}$, 250-fold less than the specific activity of $^{His}\beta\beta'$, and 0.004 Y·/$\beta_2$.

To further confirm the activity of $\beta_2$, a yeast strain was constructed, which contained *FLAG-RNR2* at the *RNR2* locus and an *rnr4*Δ deletion. The $^{Flag}\beta_2$ could be isolated from this strain in sufficient quantities to be assayed with α. This protein had a specific activity of 2 nmol min$^{-1}$ mg$^{-1}$. Thus, $\beta_2$ with either an N-terminal FLAG or His tag has low but measurable activity. These results together explain how the *rnr4*Δ strain can be viable. In this strain, a small fraction of the $\beta_2$ present has an assembled diferric-Y· cofactor. Thus, this small amount of holo-$\beta_2$ must be sufficient to support the replication of DNA in the *rnr4*Δ strain. Furthermore, the low specific activity of $\beta_2$ *in vitro* and *in vivo* supports our hypothesis that the heterodimer is the predominant form of yeast R2.

*Cotranslation of* $\beta$ *and* $\beta'$ *Is Not Required To Obtain Soluble* $\beta$ *in Vivo*. The proposal of Thelander and co-workers that $\beta'$ is a folding chaperone for $\beta$ led to the suggestion that $\beta$ and $\beta'$ need to be cotranslated to generate soluble folded $\beta\beta'$ (*8*). This hypothesis makes a prediction that $\beta_2$ expressed in the *rnr4*Δ strain has a defect in cluster assembly because of improper folding. We tested the ability of $\beta_2$ in the *rnr4*Δ strain to form a heterodimer using $^{HA}\beta'_2$ as a probe of its folding state. Increasing amounts of crude extracts from the *rnr4*Δ strain were mixed with $^{HA}\beta'_2$ (8 $\mu$g or 200 pmol of $^{HA}\beta'$). The mixture was subsequently immunoprecipitated with anti-HA agarose, and the products were analyzed by SDS−PAGE. As revealed in Figure 9, $\beta$ co-immunoprecipitated with $^{HA}\beta'$. Furthermore, as increasing amounts of *rnr4*Δ extract were added, the band corresponding to $\beta$ increased in intensity until the band for $\beta$ was roughly equal in intensity to that of $^{HA}\beta'$. Because the amount of $\beta$ present per microgram of *rnr4*Δ extract has been determined previously using quantitative Western blotting, the amount of $\beta$ present in each immunoprecipitation experiment can be estimated. The results are listed above each lane in Figure 9. These calculations reveal that the immunoprecipitation experiment shown in Lane 4 contains sufficient quantities of $\beta$ in the *rnr4*Δ extract to quantitatively form $\beta^{HA}\beta'$, and thus, a stoichiometric amount of $\beta$ co-immunoprecipitates with $^{HA}\beta'$. Because the majority of $\beta$ in the *rnr4*Δ extract is capable of generating $\beta^{HA}\beta'$, we conclude that $\beta_2$ can fold in the absence of $\beta'_2$ and is capable of forming an apo-$\beta\beta'$ if $\beta'_2$ is present. Furthermore, consistent with our *in vitro* observations, when the wt crude extract was used instead of the *rnr4*Δ extract, no $\beta$ was found to co-immunoprecipitate with $^{HA}\beta'$, thus

demonstrating that the holo-$\beta\beta'$ does not exchange its protomers (data not shown).

## DISCUSSION

Several lines of genetic and biochemical evidence have led to the proposal that the active form of the yeast R2 is $\beta\beta'$. Deletion of *RNR4* leads to the loss of viability or slow growth and cold sensitivity, suggesting an important role of $\beta'$ (*4*−*6*). Previous biochemical studies revealed that $\beta\beta'$ containing 0.3−0.4 equiv of diferric-Y· cofactor could be isolated and is active in nucleotide reduction with α (*7*, *8*). In contrast, while $\beta_2$ and $\beta'_2$ could be isolated, they had no detectable di-iron cofactor and consequently no detectable activity in the nucleotide reduction assay. While our previous studies demonstrated an interaction between $\beta$ and $\beta'$ by their co-immunoprecipitation from crude extracts, the stoichiometry between $\beta$ and $\beta'$ was not reported (*6*, *9*). All of these observations are consistent with the heterodimer model. However, they also could support a model in which $\beta'$ is needed in the assembly of diferric-Y· in $\beta$ and that reorganization of holo-$\beta\beta'$ to active $\beta_2$ requires other factors not present in the *in vitro* reconstitution experiments.

Our *in vitro* and *in vivo* results reported here further establish the relevance of the heterodimer observed *in vitro* to the active form of yeast R2 *in vivo*. Using several epitope-tagged R2s expressed in yeast under control of their endogenous promoters, we demonstrate that $\beta$ and $\beta'$ can be purified from crude cell extracts in a 1:1 molar ratio. A comparison of wt and *rnr4*Δ strains by a number of methods suggests that $\beta'$ is critical to the assembly of di-iron Y· cofactor in $\beta$. The viability of the *rnr4*Δ strains is explained by the dramatic upregulation of the concentration of $\beta$ and the ability of $\beta_2$ to self-assemble the cluster at levels that are 250-fold lower than that of the wt but sufficient for cell survival. Finally, our *in vitro* exchange reactions suggest that holo-$\beta\beta'$ is unlikely to reorganize to form active $\beta_2$.

While these results establish that $\beta\beta'$ is the active form of R2 *in vivo*, they do not define the role of $\beta'$. Thelander and co-workers have proposed that the function of $\beta'$ is to correctly fold and stabilize $\beta$ and that these two proteins must be cotranslated for efficient heterodimer formation to occur (*8*). Our results do not support this hypothesis. We observed rapid formation of the heterodimer when $^{His}\beta_2$ and $\beta'_2$ are mixed at physiological concentrations, which would not occur if $^{His}\beta_2$ was misfolded. We have also shown that apo-$^{His}\beta_2$ is unstable, a characteristic associated with all apo-R2s, and prone to aggregation and proteolysis. Thus, the exchange studies with $^{His}\beta_2$ may be disputed as the tag apparently stabilizes the protein in some fashion. However, we have also demonstrated that nontagged $\beta_2$ present in crude extracts generated from a *rnr4*Δ strain is capable of participating in the same exchange reaction to form the heterodimer, further supporting the relevance of our exchange reaction studies *in vitro*. Moreover, we have established that most of $\beta_2$ present in the crude extract is capable of forming a heterodimer with $\beta'_2$, arguing against a model that only a small fraction of $\beta_2$ is properly folded. The cells have some mechanism to stabilize apo-$\beta_2$ in the absence of $\beta'$ in the *rnr4*Δ. These data together suggest that cotranslation of $\beta$ and $\beta'$ is not essential.

Previously, we have proposed that $\beta'_2$ is a catalytic iron chaperone, required transiently in the cofactor assembly of $\beta_2$, similar to the role proposed for Ccs1, the copper chaperone for copper zinc superoxide dismutase (*10*−*12*). However, our previous findings that $\beta'_2$ was needed in stoichiometric amounts to activate $\beta_2$ and that no iron could be detected bound to $\beta'_2$ are inconsistent with this proposal (*7*). Furthermore, the results presented here demonstrate that $\beta\beta'$ is the predominant species *in vivo*, which does not support the proposal that $\beta'_2$ is needed catalytically in the activation of $\beta$.

Our recent structures of $^{His}\beta_2$, $\beta'_2$, and $^{His}\beta\beta'$ have suggested an alternative role for $\beta'$ to stabilize a local conformation of $\beta_2$ that would promote cofactor assembly (*13*, *14*). Specifically, helix αB of $\beta_2$, harboring the di-iron cluster ligand Asp145, becomes ordered upon heterodimer formation. The observation that the *rnr4*Δ strain overexpresses $\beta_2$ by 15-fold yet has significantly less Y· and RNR activity than the wt strain supports the hypothesis that $\beta'$ is required for the cofactor assembly in $\beta\beta'$ *in vivo*. Furthermore, our observations that tagged-$\beta_2$ can assemble small amounts of the cofactor in the absence of $\beta'$ supports our hypothesis that a majority of $\beta_2$ in solution is in a conformation that cannot efficiently assemble the cofactor.

As we learn more about the insertion of metals into enzyme active sites *in vivo*, it is becoming clear that in the case of copper, nickel, zinc, and iron (for iron−sulfur clusters), metallochaperones are required to deliver the metal and perhaps required reducing equivalents in a regulated fashion to assemble holo-metalloproteins (*10*, *27*, *28*). Perhaps the role of $\beta'$ *in vivo* is to stabilize $\beta$ to allow for cofactor assembly as proposed above or to facilitate interactions with the cellular machinery required for cofactor insertion. We have shown with the *rnr4*Δ strain studies that the cell must sense this defect in RNR activity, likely through activation of the DNA damage checkpoint by replicational stress resulting from low concentrations of deoxynucleotides (*29*, *30*), and responds to it through upregulation of α and α′ concentrations in addition to a dramatic upregulation of the $\beta$ concentration. Perhaps, the cell also upregulates the machinery required for cofactor insertion, thus setting the stage for us to use this strain to search for the RNR iron chaperone protein(s).

## REFERENCES

1. Jordan, A., and Reichard, P. (1998) Ribonucleotide reductases, *Annu. Rev. Biochem. 67*, 71−98.
2. Elledge, S. J., and Davis, R. W. (1987) Identification and isolation of the gene encoding the small subunit of ribonucleotide reductase from *Saccharomyces cerevisiae*—DNA damage-inducible gene required for mitotic viability, *Mol. Cell. Biol. 7*, 2783−2793.
3. Hurd, H. K., Roberts, C. W., and Roberts, J. W. (1987) Identification of the gene for the yeast ribonucleotide reductase small subunit and its inducibility by methyl methanesulfonate, *Mol. Cell. Biol. 7*, 3673−3677.
4. Winzeler, E. A., Shoemaker, D. D., Astromoff, A., Liang, H., Anderson, K., Andre, B., Bangham, R., Benito, R., Boeke, J. D., Bussey, H., Chu, A. M., Connelly, C., Davis, K., Dietrich, F., Dow, S. W., El Bakkoury, M., Foury, F., Friend, S. H., Gentalen, E., Giaever, G., Hegemann, J. H., Jones, T., Laub, M., Liao, H., Liebundguth, N., Lockhart, D. J., Lucau-Danila, A., Lussier, M., M'Rabet, N., Menard, P., Mittmann, M., Pai, C., Rebischung, C., Revuelta, J. L., Riles, L., Roberts, C. J., Ross-MacDonald, P., Scherens, B., Snyder, M., Sookhai-Mahadeo, S., Storms, R. K., Veronneau, S., Voet, M., Volckaert, G., Ward, T. R., Wysocki, R., Yen, G. S., Yu, K. X., Zimmermann, K., Philippsen, P., Johnston, M., and Davis, R. W. (1999) Functional characterization

of the *S. cerevisiae* genome by gene deletion and parallel analysis, *Science 285*, 901−906.
5. Wang, P. J., Chabes, A., Casagrande, R., Tian, X. C., Thelander, L., and Huffaker, T. C. (1997) Rnr4p, a novel ribonucleotide reductase small-subunit protein, *Mol. Cell. Biol. 17*, 6114−6121.
6. Huang, M. X., and Elledge, S. J. (1997) Identification of RNR4, encoding a second essential small subunit of ribonucleotide reductase in *Saccharomyces cerevisiae*. *Mol. Cell. Biol. 17*, 6105−6113.
7. Ge, J., Perlstein, D. L., Nguyen, H. H., Bar, G., Griffin, R. G., and Stubbe, J. (2001) Why multiple small subunits (Y2 and Y4) for yeast ribonucleotide reductase? Toward understanding the role of Y4, *Proc. Natl. Acad. Sci. U.S.A. 98*, 10067−10072.
8. Chabes, A., Domkin, V., Larsson, G., Liu, A. M., Graslund, A., Wijmenga, S., and Thelander, L. (2000) Yeast ribonucleotide reductase has a heterodimeric iron-radical-containing subunit, *Proc. Natl. Acad. Sci. U.S.A. 97*, 2474−2479.
9. Nguyen, H. H. T., Ge, J., Perlstein, D. L., and Stubbe, J. (1999) Purification of ribonucleotide reductase subunits Y1, Y2, Y3, and Y4 from yeast: Y4 plays a key role in diiron cluster assembly, *Proc. Natl. Acad. Sci. U.S.A. 96*, 12339−12344.
10. Finney, L. A., and O'Halloran, T. V. (2003) Transition metal speciation in the cell: Insights from the chemistry of metal ion receptors, *Science 300*, 931−936.
11. Huffman, D. L., and O'Halloran, T. V. (2001) Function, structure, and mechanism of intracellular copper trafficking proteins, *Annu. Rev. Biochem. 70*, 677−701.
12. Rae, T. D., Schmidt, P. J., Pufahl, R. A., Culotta, V. C., and O'Halloran, T. V. (1999) Undetectable intracellular free copper: The requirement of a copper chaperone for superoxide dismutase. *Science 284*, 805−808.
13. Sommerhalter, M., Voegtli, W. C., Perlstein, D. L., Ge, J., Stubbe, J., and Rosenzweig, A. C. (2004) Structures of the yeast ribonucleotide reductase Rnr2 and Rnr4 homodimers, *Biochemistry 43*, 7736−7742.
14. Voegtli, W. C., Ge, J., Perlstein, D. L., Stubbe, J., and Rosenzweig, A. C. (2001) Structure of the yeast ribonucleotide reductase Y2Y4 heterodimer, *Proc. Natl. Acad. Sci. U.S.A. 98*, 10073−10078.
15. Yao, R. J., Zhang, Z., An, X. X., Bucci, B., Perlstein, D. L., Stubbe, J., and Huang, M. X. (2003) Subcellular localization of yeast ribonucleotide reductase regulated by the DNA replication and damage checkpoint pathways, *Proc. Natl. Acad. Sci. U.S.A. 100*, 6628−6633.
16. Sikorski, R. S., and Hieter, P. (1989) A system of shuttle vectors and yeast host strains designed for efficient manipulation of DNA in *Saccharomyces cerevisiae*, *Genetics 122*, 19−27.
17. Elledge, S. J., Richman, R., Hall, F. L., Williams, R. T., Lodgson, N., and Harper, J. W. (1992) Cdk2 encodes a 33-kDa cyclin-A-associated protein kinase and is expressed before Cdc2 in the cell cycle, *Proc. Natl. Acad. Sci. U.S.A. 89*, 2907−2911.
18. Longtine, M. S., McKenzie, A., Demarini, D. J., Shah, N. G., Wach, A., Brachat, A., Philippsen, P., and Pringle, J. R. (1998) Additional modules for versatile and economical PCR-based gene deletion and modification in *Saccharomyces cerevisiae*, *Yeast 14*, 953−961.
19. Bollinger, J. M., Tong, W. H., Ravi, N., Huynh, B. H., Edmondson, D. E., and Stubbe, J. (1995) Use of Rapid Kinetics Methods to Study the Assembly of the Diferric-Tyrosyl Radical Cofactor of *Escherichia coli* Ribonucleotide Reductase, in Redox-Active Amino Acids in Biology, pp 278−303.
20. Perlstein, D. L., Robblee, J., Huang, M. X., and Stubbe, J. (2005) Quantitation of metallocofactor stoichiometry *in vivo*—Isolation of yeast's endogenous ribonucleotide reductase small subunit, *Biochemistry*, in preparation.
21. Jorgensen, P., Nishikawa, J. L., Breitkreutz, B. J., and Tyers, M. (2002) Systematic identification of pathways that couple cell growth and division in yeast, *Science 297*, 395−400.
22. Gietz, R. D., and Schiestl, R. H. (1995) Transforming yeast with DNA, *Method Mol. Cell. Biol. 5*, 255−269.
23. Steeper, J. R., and Steuart, C. D. (1970) A rapid assay for CDP reductase activity in mammalian cell extracts, *Anal. Biochem. 34*, 123−130.
24. Dyson, H. J., and Wright, P. E. (2005) Intrinsically unstructured proteins and their functions, *Nat. Rev. Mol. Cell Biol. 6*, 197−208.
25. Lammers, M., and Follmann, H. (1984) Deoxyribonucleotide biosynthesis in yeast (*Saccharomyces cerevisiae*) a ribonucleotide reductase system of sufficient activity for DNA synthesis, *Eur. J. Biochem. 140*, 281−287.
26. Harder, J., and Follmann, H. (1990) Identification of a free-radical and oxygen dependence of ribonucleotide reductase in yeast, *Free Radical Res. Commun. 10*, 281−286.
27. Kuchar, J., and Hausinger, R. P. (2004) Biosynthesis of metal sites, *Chem. Rev. 104*, 509−525.
28. Rosenzweig, A. C., and O'Halloran, T. V. (2000) Structure and chemistry of the copper chaperone proteins, *Curr. Opin. Chem. Biol. 4*, 140−147.
29. Elledge, S. J., Zhou, Z., Allen, J. B., and Navas, T. A. (1993) DNA damage and cell cycle regulation of ribonucleotide reductase, *BioEssays 15*, 333−339.
30. Zhou, B. B. S., and Elledge, S. J. (2000) The DNA damage response: Putting checkpoints in perspective, *Nature 408*, 433−439.

BI051616+